Environmental Pollution 345 (2024) 123524

Contents lists available at ScienceDirect

Environmental Pollution

journal homepage: www.elsevier.com/locate/envpol

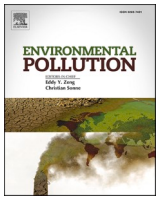

Plastic does not simply flow into the sea: River transport dynamics affected by tides and floating plants☆

R.A. Lotcheris [a,b,*], L.J. Schreyers [b], T.K.L. Bui [c], K.V.L. Thi [b,d], H.-Q. Nguyen [c], B. Vermeulen [b], T. H.M. van Emmerik [b]

[a] Stockholm Resilience Centre, Stockholm University, Stockholm, Sweden
[b] Hydrology and Environmental Hydraulics, Wageningen University, Wageningen, the Netherlands
[c] Institute for Circular Economy Development, Vietnam National University, Ho Chi Minh City, Viet Nam
[d] Faculty of Water Resources, Hanoi University of Natural Resources and Environment, Hanoi, Viet Nam

ARTICLE INFO

Keywords:
Macroplastic
Water quality
Plastic pollution
Water hyacinths
Saigon
Estuary
Pollution transport
Marine debris
Stopping and re-mobilization
Hydrology
Vietnam

ABSTRACT

Plastic pollution is ubiquitous in aquatic environments worldwide. Rivers connect terrestrial and marine ecosystems, playing a key role in the transport of land-based plastic waste towards the sea. Emerging research suggests that in estuaries and tidal rivers, tidal dynamics play a significant role in plastic transport and retention dynamics. To date, observations in these systems have been limited, and plastic transport dynamics during single tidal cycles remain poorly understood. Here, we investigated plastic transport, trapping, and re-mobilization of macroplastics (> 0.5 cm) in the Saigon River, focusing on short-term dynamics of individual tidal cycles. We used GPS trackers, released at different stages of the tidal cycle (ebb, flood, neap, spring). Plastic items demonstrated dynamic and intermittent transport behavior. Items spent almost half of the time (49%) temporarily stopped, mainly due to their entrapment in vegetation, infrastructure, or deposition on riverbanks. Items were almost always re-mobilized within 10 h (85%), leading to successive phases of stopping and transport. Tidal dynamics also resulted in bidirectional transport of plastic items, with median daily total transport distance within the 40 km study reach (8.9 km day^{-1}) over four times larger than the median daily net distance (2.0 km day^{-1}). The median retention time of plastic items within the reach was 21 days (mean = 202 days). In total, 81% of the retrieved items were trapped within water hyacinths, emphasizing the important role of floating vegetation on river plastic transport dynamics. With this paper, we aim to provide data-driven insights into macroplastic transport and retention dynamics in a tropical tidal river. These are crucial in the design of effective intervention and monitoring strategies, and estimating net plastic emission from rivers into the sea.

1. Introduction

Plastic pollution in global rivers is of growing concern due to its direct negative effects on the riverine environment, and because of its emissions into the oceans (Jambeck et al., 2015). Recent estimates suggest that over a thousand rivers emit a combined 0.8 to 2.7 million metric tons into the ocean each year (Meijer et al., 2021). Hydrology is thought to play a crucial role in the transport processes of plastic pollution through river systems, and discharge has been found to correlate strongly with river plastic transport, especially during (extreme) flood events (van Emmerik et al., 2022a; Roebroek et al., 2021; van Emmerik et al., 2023). However, the exact relationships between hydrological variables and plastic transport dynamics are non-linear, and variable over time and space. Especially in hydrologically complex areas, such as confluences, bifurcations, and tidal river reaches, the governing processes that drive plastic transport and retention dynamics remain unresolved. This in turn leads to large uncertainties of local, regional, and global estimates of river plastic transport and emissions into the sea (Roebroek et al., 2022). Field-based observations are therefore crucial to improve the fundamental understanding of plastic transport.

Hydrological processes in tidal rivers are complicated by the combined influence of the tide and freshwater discharge (Savenije, 2006). Water level, flow velocity, and flow direction change diurnally, which

☆ This paper has been recommended for acceptance by Dr Michael Bank.

* Corresponding author. Stockholm Resilience Centre, Stockholm University, Stockholm, Sweden.
E-mail address: romi.lotcheris@su.se (R.A. Lotcheris).

https://doi.org/10.1016/j.envpol.2024.123524
Received 9 May 2023; Received in revised form 20 December 2023; Accepted 6 February 2024
Available online 12 February 2024

can in turn impact the transport and retention of plastics (Tramoy et al., 2020a; Valero et al., 2022). Recent research has suggested that tidal and estuarine zones play an important role in the retention of macroplastics in rivers (Duncan et al., 2020; Tramoy et al., 2020b,a; Ledieu et al., 2022; van Emmerik et al., 2022b).

The bidirectional flow increases the likelihood of plastic stranding on riverbanks, or trapping in vegetation and sediment. Other studies found higher sediment and riverbank plastic density in the tidal zone of rivers compared to the non-tidal zones (Acha et al., 2003; van Emmerik et al., 2020). Both Eulerian and Lagrangian methods have been used to study plastic transport. Examples include net sampling or visual counting from bridges to determine the net transport at specific locations in a river system (van Emmerik et al., 2020; Blondel and Buschman, 2022). Lagrangian methods have used drifters both with- and without GPS systems to study the movement of individual items, revealed limited net transport, and high retention on riverbanks and in vegetation (Ledieu et al., 2022; Tramoy et al., 2020a; Mani et al., 2023). Although these studies have demonstrated the role of tidal zones in retaining plastics for longer time scales (weeks to months), their longer temporal scope with lower frequency measurements mean the transport dynamics during at sub-daily time-scales remain unresolved.

In this paper we use high-frequency (10 s) observations of tracked macroplastic items in the Saigon River, Vietnam, to demonstrate that rivers are not just conduits for land-based plastic waste into the sea. Instead, plastics interact strongly with river system features and are affected by tidal dynamics, leading to high probabilities of being retained on short time-scales. Current river plastic export models (Meijer et al., 2021; Nakayama and Osako, 2023) do not take these dynamics into account, suggesting that the global input of plastic from rivers into the ocean may be overestimated. Further research on the fundamental transport and retention dynamics in tidal rivers is crucial to improve and parameterize plastic models, provide guidance on how to optimize plastic waste prevention and reduction strategies, and help determine the timing and magnitude of pollution events.

2. Methodology

2.1. Study area

Ho Chi Minh City (HCMC) is the largest city in Vietnam with a population of over 8 million people (Lahens et al., 2018). Rapid urbanisation and industrial development have made effective waste management an ongoing challenge for the city's municipal waste institutions (Nguyen et al., 2021). The Saigon River acts as a conduit for mismanaged plastic, with an estimated 0.35–7.3 kg of plastic waste per inhabitant entering the river each year (Lahens et al., 2018).

The Saigon River is 250 km long and drains a catchment area of 4717 km^2, with discharge varying seasonally between a few tens of m^3 s^{-1} and 1500 m^3 s^{-1} (Nguyen et al., 2021; Camenen et al., 2021). The Southern Vietnamese climate is dominated largely by the seasonally reversing monsoon circulation. This results in a large variation in discharge between the dry (December to April) and wet (May to November) seasons. The mean annual discharge is estimated to be approximately 50 m^3 s^{-1} (Nguyen et al., 2021). During the study period, the river experiences an asymmetrical, mixed semi-diurnal tidal regime with a tidal amplitude of 2 m, typically resulting in flow reversal twice

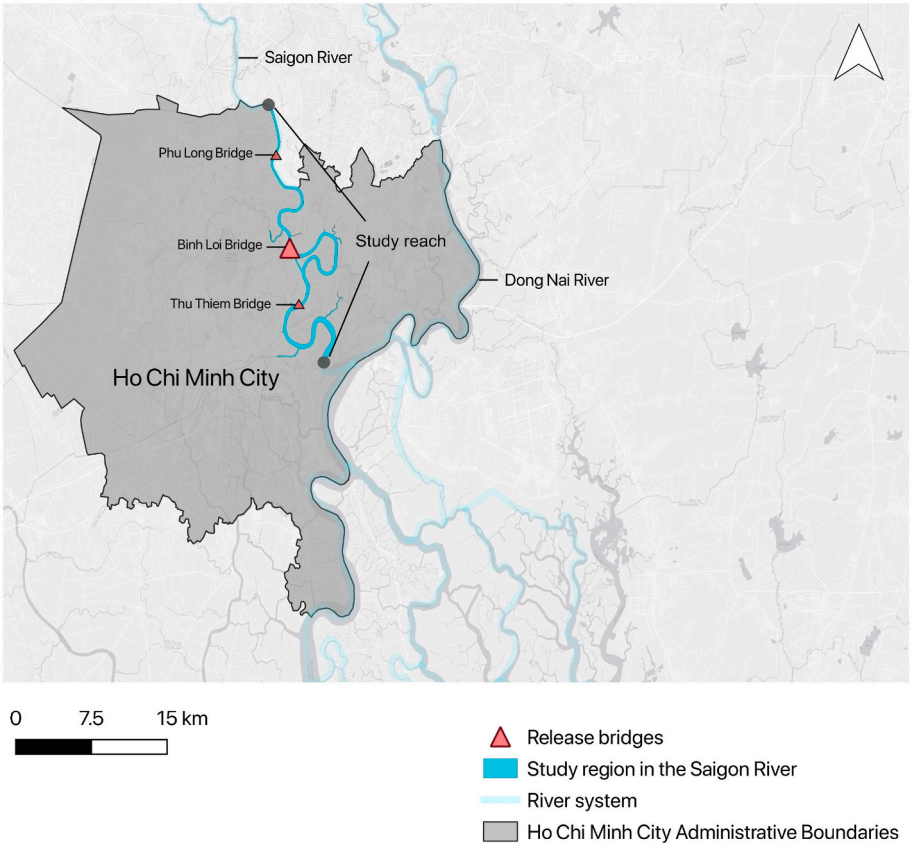

Fig. 1. The study area shown in the context of Ho Chi Minh City and surrounding areas in Southern Vietnam. The boundaries of the study reach are indicated, with a total length of 40 km. The release bridges (Phu Long bridge (number of releases (n) = 3), Binh Loi bridge (n = 53), and Thu Thiem (n = 2) bridge) are highlighted with a red triangle. Most trackers were released from Binh Loi bridge (n = 53), which is indicated by a larger triangle. Water pressure measurements were carried out at Binh Loi bridge and Phu Long bridge. City boundary shapefiles obtained from: https://gadm.org/data.html; river shapefiles from: https://www.hydrosheds.org/. (For interpretation of the references to color in this figure legend, the reader is referred to the Web version of this article.)

Table 1
Metrics of stopping and transport extracted from trajectory data.

Metric	Unit	Description
Net transport velocity	[km day^{-1}]	Distance from the release location to the location of retrieval calculated separately for trajectories with either a net upstream or a net downstream travel direction
Total transport velocity	[km day^{-1}]	Full length of trajectory, including back and forth transport within the system
Re-mobilization probability	[-]	Items with a number of stops greater than one (see Appendix A)
Residence time	[days]	Ratio between the system length and the transit time through the system
Trajectory duration	[hrs]	Total time a particle spent in the system, excluding missing data (see Appendix A)
Time spent stopped	[hrs]	Total time a particle spent stopped while in the system
Mean duration of stops	[hrs]	The average stop duration for all stops in a trajectory
Time to first stop	[hrs]	Elapsed time from the moment of release to the first detected stop
Number of stops per hour	[n/hr]	Number of detected stops over the length of the trajectory
Stopped time/total time	[-]	Proportion of time an items spends stopped with respect to the total trajectory length

daily. The Saigon River is affected by invasive floating water hyacinths, which can cover up to 25% of the total river surface (Janssens et al., 2022).

Trackers were released primarily from the Binh Loi bridge (10.825698°N, 106.709175°E, number of items (n) = 53) in the centre of the study area. A small number were also released from Phu Long bridge (10.890252°N, 106.692063°E, n = 3) upstream, and Thu Thiem bridge (10.786274°N, 106.718091°E, n = 2) in the city centre, downstream (Fig. 1). The study area begins 5 km upstream of the upstream bridge, accounting for the items released at this bridge, and ends at the confluence to the Dong Nai River. This yields a 40 km long reach (Fig. 1). Trackers travelling beyond either the up- or downstream boundary were considered to have left the system. The study reach is in a low elevation zone, between 0 and 10 m, and has a high sinuosity (sinuosity ≈ 2) with several large meanders directly downstream from the central and primary release bridge, Binh Loi bridge. An artificial channel has been constructed directly downstream from this release bridge which circumvents one of these meanders. This presents two potential pathways a plastic item could travel (Fig. 1).

2.2. Data collection

2.2.1. Tracker experiments

The data for this research were collected in the Saigon River in Ho Chi Minh City from the May 7, 2022 to the June 15, 2022, where we conducted 58 tracker experiments. To replicate the movements of macroplastic items in the Saigon River, GPS trackers (87 × 54 × 26 mm; see Appendix A for details) were placed into macroplastic items and tracked over the course of one or more tidal cycles. Trackers were fixed inside an expanded polystyrene (EPS) box (20 × 15 × 15 cm). EPS items are among the most frequently found items in the Saigon River, as well as in other rivers, beaches, and marine waters across South-East Asia. The size and properties of plastic items used in this study therefore reflect typical items in the Saigon River (Lahens et al., 2018; van Emmerik et al., 2019; Chan and Not, 2023). EPS items have a low density, between 0.016 and 0.640 g cm^{-3}, resulting in high buoyancy (van Emmerik and Schwarz, 2020). This buoyancy meant the trackers were also affected by wind.

For each tracker experiment, four to six trackers were released at the same locations at the mid-point of the release bridges. Trackers (n = 58) were released at different times to cover the full range of tidal conditions for short time-scales (sub-daily to weekly; ebb: 41%; n = 24), flood 59%; n = 34 flood, spring: 47%; n = 27, neap: 53%; n = 31). Trackers remained in the system for at least one tidal cycle (24 h and 50 min). Trackers were deployed for an average time period of 2.5 ± 3 days (median = 1.5 days). After removing missing data (see 2.3.1) the longest trajectory duration was just over 16 days. The shortest trajectory was 4.2 h. Trackers reported their position every 10 s when in motion, or every hour when stopped. For brevity, we refer to the GPS tracker set-up in the EPS box as the 'item' for the remainder of this paper.

2.2.2. Hydrological measurements and tidal analysis

Water pressure data loggers were installed at the downstream (Thu Thiem) and centre (Binh Loi) bridges, to estimate water level for the study period (Appendix B). Data loggers were placed close to riverbanks for accessibility reasons, which sometimes caused the water level to drop below the submerged diver during spring tides. The observed water level time-series were therefore used in a harmonic analysis using the *T tide* package for MATLAB (Pawlowicz et al., 2002). The modelled water level was used for the remainder of the analysis to determine both the tidal phase (spring/neap) and the tidal state (flood/ebb/slack) during the tracker experiments. A phase shift between minimum flow velocity and maximum water level was found to be 1 h and 36 min, which was added to the start and end periods of flood and ebb. For details regarding the tidal analysis, refer to Appendix B).

2.3. Processing and analysis

2.3.1. Pre-processing

Item trajectories are comprised of a series of points with longitude, latitude, and a timestamp. The tracking device sent a signal every 10 s when the device was in motion, or every hour when no movement was detected. An item was considered to have stopped when it remained within a 30 m radius for longer than 30 min to account for erroneous signals. Poor signal due to poor satellite coverage, being shielded by vegetation or infrastructure, being partially submerged, or heavy precipitation and cloud cover could result in long intervals between points (up to 5 days in one case). The handling of trajectory gaps is detailed in Appendix A.

2.3.2. Metrics of transport and trapping

The detection of stops was done using the Moving Pandas package (Version 0.11) by Graser (2019). From the detected stops, several metrics were extracted, shown in Table 1. The probabilities of stopping and re-mobilization within time t (P_t) are defined as the time since release that an item stops, and the time since the start of a stop that an item begins moving again, respectively. Both these metrics have a probability density function that takes the shape of an exponential, described as:

$$P_t = 1/\beta exp(-t/\beta) \quad (1)$$

Where the shape parameter β is the respective mean of the time to first stop and time to re-mobilization for all trajectories (β = 2.5 h), and for trajectories separated by release conditions (spring: β = 2.5 h; neap: β = 2.7 h; flood: β = 2.42 h; ebb: β = 1.8 h). Probability density functions were fitted based on the histograms of the times to first stop and times to re-mobilization (Appendix D.7). The probability of stopping and re-mobilization events occurring within a defined time can then be estimated from the cumulative density function.

Metrics of transport are the net distance and the total distance travelled (Table 1), calculated in QGIS (Version 3.22). The net distances were calculated and reported separately for items with a net upstream travel direction and for those with a net downstream travel direction.

The total distance is the entire distance travelled by the item from the moment of release to the moment of retrieval. Because the length of time in the system could vary, both net and total distance are expressed as the net daily average transport velocity (up- and downstream) and total daily average transport velocity in kilometers per day.

To set the net velocity in the context of the system, we provide a first order estimate of the residence time as an indication of the total time it takes for an item to leave the study reach. Residence time, or flushing time, is given by the ratio between the volume of a system and the volumetric flow rate through the system (Valle-Levinson, 2010 p. 278; Monsen et al., 2002). In our analysis, the ratio between the length of system (40 km) and the net travel velocity was used:

$$t_r = \frac{d_{system}}{|(v_{net})|} \quad (2)$$

Where t_r is the residence time, d_{system} is defined as the total length of the river system in the study area, and v_{net} is the net transport velocity.

There are several terms used in the analysis of the results to refer to the different processes of transport and stopping. For clarity, we illustrate these terms in Appendix D.6. Here, transport refers to the mobile phase of a trajectory and stopping to the immobile phase. Both stopping and transport can occur while an item is associated with floating vegetation. Trapping refers to an item which has become trapped in, for example, riparian vegetation, floating vegetation, docks, ships, bridge infrastructure, improvised embankments, or under platforms. An item is defined to have stopped when it remains within a 30 m radius for longer than 30 min. Note that an item can become trapped by floating vegetation, but still remain in motion. An item can also be deposited on the riverbank. Re-mobilization can occur from any of these environments, when an item is once again mobile and being transported. In a tidal river, transport can be both in the upstream and downstream directions, and as such, an item is exported out of the system when it leaves either the upstream or downstream system boundaries. Several example trajectories are shown in Appendix D.13.

2.3.3. Statistical analysis

Statistical analyses were used to test for relationships between the abovementioned metrics and the tidal conditions. Shapiro-Wilk tests for normality revealed none of the metrics were normally distributed. Because of this, and the relatively small sample sizes (< 60), non-parametric Mann-Whitney U tests were used to test for significant relationships between metrics (see Table 1) and the tidal release conditions (spring vs. neap and flood vs. ebb). For categorical metrics and variables (tide phase, tide state, location found, net transport direction), a Chi-Squared test was used. The p-value was set at p = 0.05, where anything below this value was deemed significant.

Table 2
Probabilities of stopping (P_S) and remobilization (P_R) for particles released under different tidal release conditions, and probability densities of stopping within 1, 3, and 10 h. The probability of stopping indicates the state of the tide when the item was released, not at the moment of re-mobilization. In the case of the flood and ebb tidal phases, these are distinct.

Release condition	P_S	P_S, T 1hr	P_S, T < 3hr	P_S, T < 10hr
All	0.97	0.37	0.75	0.99
Spring	1.00	0.36	0.74	0.99
Neap	0.94	0.37	0.75	0.99
Flood	0.97	0.34	0.71	0.98
Ebb	0.96	0.42	0.81	1.00
Release condition	P_R	P_R,T < 1hr	P_R,T < 3hr	P_R, T < 10hr
All	0.93	0.17	0.43	0.85
Spring	1.00	0.18	0.45	0.86
Neap	0.86	0.17	0.42	0.84
Flood	0.90	0.17	0.42	0.84
Ebb	0.95	0.18	0.44	0.86

3. Results

3.1. Nearly all items stop within 10 h of transport

Nearly all items released in the Saigon River (97%) stopped at least once during their trajectories in the river (Table 2). For all trajectories, the mean time to first stop was 2.5 h (median = 1.1 h). Most items stopped quickly after their release in system (37% within 1 h, and 75% within 3 h, (Table 2; Appendix D.8A). Almost all items (99%) stopped within 10 h after their release. Note that of all the recorded stops, just 15% took place during a slack water period. Because stopping occurs rapidly once items have been released, studying the mechanisms at short-time scales, (hourly - weekly) is highly relevant in riverine environments.

There is no significant difference between spring and neap tides, which act over longer timescales, regarding the time to first stop (Appendix D.8A). The median time to first stop for items released during both spring and neap tides is 1.1 h (mean = 2.7 h and 2.4 h, respectively). The difference in time to first stop during ebb (2.4 h) and flood (1.8 h) releases is more noticeable (Appendix D.8A and Appendix C).

The state of the tide at the moment an item is released into the river system may thus play an important role in systematically transporting items towards or away from regions where items might preferentially become trapped, while simultaneously increasing or decreasing the potential exposure to these environments. Items might be more readily trapped downstream of the release location than upstream. The downstream section is less channelised and has more exposed riparian vegetation and riverine infrastructure, all of which increase shoreline roughness. A decrease in water level during the ebb tide may also increase exposure to trapping environments.

Remarkably, 81% (n = 47) of retrieved items were found trapped within hyacinth patches (Fig. 2A). We found a significant relationship between the tidal conditions and the location of items retrieval (p = 0.014). Almost all items found on riverbanks (90%, n = 10) were retrieved during spring tides. This could be attributed to a greater rise in water levels during the spring tides compared to the neap tides increasing the likelihood of deposition on riverbanks. There was a clear difference in items trapped at infrastructure between downstream and upstream retrieval sites clear, with 84% (n = 16) of items retrieved trapped in infrastructure downstream of the release location, and 16% (n = 3) trapped in infrastructure upstream. Fig. 2A shows the locations of every stop in the 58 trajectories, illustrating that stops tend to be close to the release location and associated with meanders. The Saigon River has a high sinuosity (sinuosity index ≈ 2). Trapping tended to occur more frequently (65%) on the outer bend of meanders compared to the inner bends (35%). This was even more pronounced for the large meanders directly downstream of the main release location (72% of trapping occurred in outer bends, 28% in inner bends). The higher trapping found on the outer bends could also be caused by wind direction, or by a higher density in trapping environments (especially infrastructure) on the side of the city (west), in the case of the downstream section.

3.2. Succession of transport, stopping and re-mobilization phases

Stopping phases can correspond to either trapping (e.g. on hyacinth patches or riverbanks) or the absence of flow during, for example, the slack phase of the tidal cycle. We found that these stopping mechanisms are largely temporary, and items are almost always re-mobilized. This makes river plastic trajectories highly dynamic and intermittent in nature, with successive periods of transport, stopping and re-mobilization. On average, items spent 49% of their time in the river stopped, and thus the remaining 51% in motion (Table B1). Items stopped on average 1.6 times per tidal cycle (0.124 times per hour). The tidal release conditions, whether ebb/flood and spring/neap, did not significantly affect any of the metrics of stopping: the ratio of time spent stopped to the total trajectory time (p-values > 0.05); the number of stops per cycle (p-

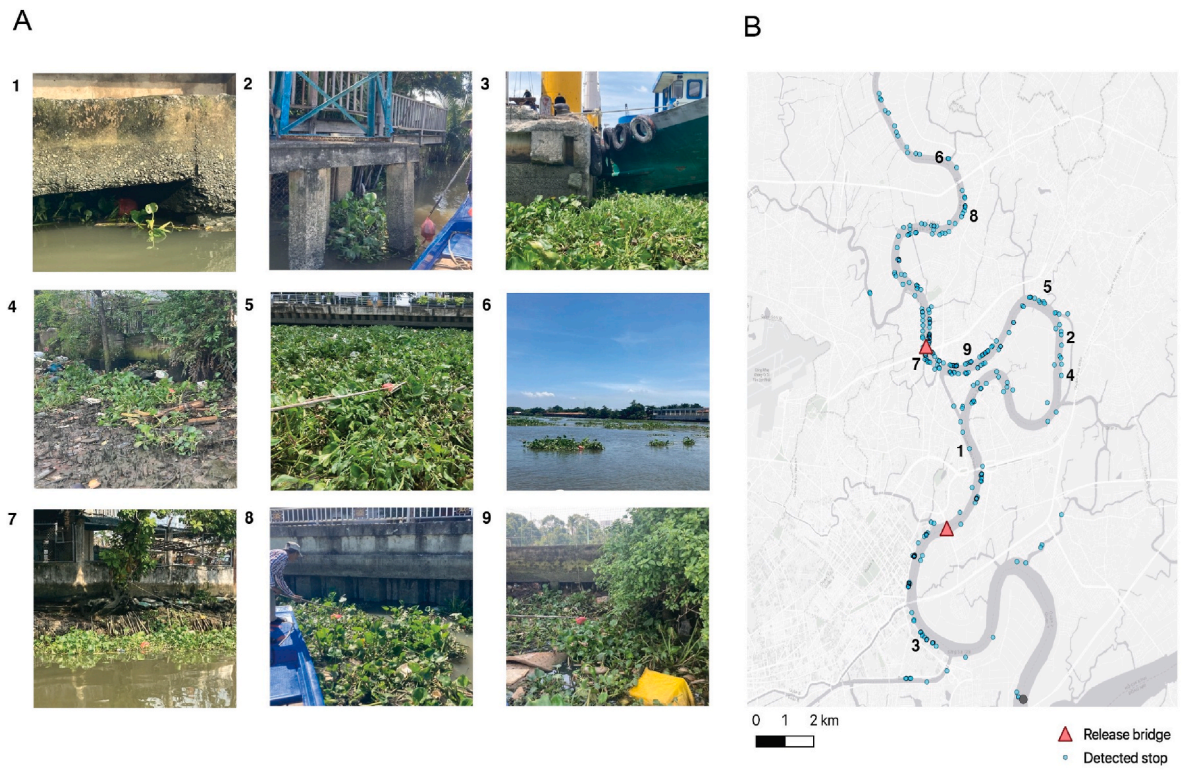

Fig. 2. A) Example locations where tracked items (red bag) were retrieved. Figures (1) - (3) items retrieved at hydrological infrastructure sites; (1) at a platform, (2) at a dock, and (3) at a docked boat. Figures (4)–(6) illustrate items retrieved in different sections of the channel; on the river bank (4), near the channel edge (5), and in the centre of the channel (6). Figures (7)–(9) show items trapped in improvised embankments (7), near channelised channel edges (8), and in riparian vegetation (9). Note here that hyacinth patches were present at all retrieval sites in these examples. B) Spatial distribution of all detected stops across all 58 trajectories. The left panel shows the entire system length, with the release sites given in red. Note the higher densities of stops on outer meanders. The highest densities of stops were within 5 km of the release site. (For interpretation of the references to color in this figure legend, the reader is referred to the Web version of this article.)

values > 0.05) and the mean stop duration (pvalues > 0.05) (Appendix D.12). While not statistically significant, spring tides were characterized by shorter stop durations (6 h 21 m in spring, 10 h 18 m in neap; $p = 0.45$) and a slightly higher number of stops per tidal cycle (1.51 and 1.54 for spring and neap, respectively, $p = 0.19$) compared to neap tides (Appendix C). This could indicate an increased re-mobilization effect during spring tides.

Most items (93%) were re-mobilized at least once in their trajectory (Table 2). The tide at release had limited effect on re-mobilization probabilities, with values ranging between 0.86 for neap releases and 1 for spring releases. Releases during spring tides had slightly higher probabilities of remobilization compared to neap conditions (1.0 and 0.85, respectively), suggesting that items released during the spring phase have a more intermittent mode of transport. Items stopped slightly more often, for shorter durations, and were more often re-mobilized than during neap. Just 3% of items were transported without ever stopping ($n = 2$, with trajectory durations of 1.8 days and 12 h), highlighting that (temporary) retention mechanisms of plastics are widespread even at the short (sub-daily and weekly) time-scales investigated.

The probabilities of re-mobilization are lower than those of stopping, indicating that during the time-frame of our experiments, there is a net retention of items within the river system. Within the first hour of transport, stopping and re-mobilization probabilities are 0.37 and 0.17, respectively (Table 2). Because stopping and re-mobilization are not equally likely, the conditions required for re-mobilisation appear distinct from those that lead to stopping, which are more easily met. Different rivers, discharge conditions, and also trapping environments within the same river reach, may therefore exhibit different patterns of transport and successive trapping and re-mobilisation. Fig. 3, presents an empirical model of the first stopping and re-mobilization of a plastic item after it has been released into a river, where the probabilities are based on the observations in the Saigon River.

3.3. Transport velocities and residence time distribution

Items had limited net daily transport velocities and stayed within the system boundaries rather than being exported, driven primarily by the bidirectional flow. More items travelled downstream of their release site than upstream (62% of items travelled downstream, Appendix C). The magnitude of the net velocity was similar between upstream and downstream directions. Items travelled an average of 4.2 km day^{-1} in the downstream direction and 4.0 km day^{-1} in the upstream direction (median net velocity = 2.0 km day^{-1} and 1.6 km day^{-1} for downstream and upstream directions, respectively). Approximately 70% of item trajectories were shorter than 5.0 km day^{-1}. Only for a few trajectories (23% and 28%, for upstream and downstream transport, respectively) was the net velocity larger than 5 km day^{-1}. On average, the total transport velocity was twice as long as the net velocity (mean total velocity = 8.9 km day^{-1}) (Appendix D.11C). Median total velocities were 3–4 times longer than net velocities (median total velocity = 6.5 km day^{-1}). The item with the smallest net velocity of just 0.0061 km day^{-1} (6.1 m day^{-1}), still had a total velocity of 5.9 km day^{-1}.

On shorter, diurnal timescales, the direction of the tidal flow at the moment of release is significantly related to the ultimate net direction of transport. Flood tides lead to a higher proportion of net upstream transport (50%), whereas ebb tides lead to a higher proportion of net downstream transport (66%). Trajectories that resulted in net upstream velocities were more than two times larger during neap than spring tide (5.3 km day^{-1} and 2.0 km day^{-1}, respectively) and close to four times larger during flood than ebb tide (4.7 km day^{-1} and 1.3 km day^{-1}, respectively) (Appendix C), indicating that tidal conditions can affect

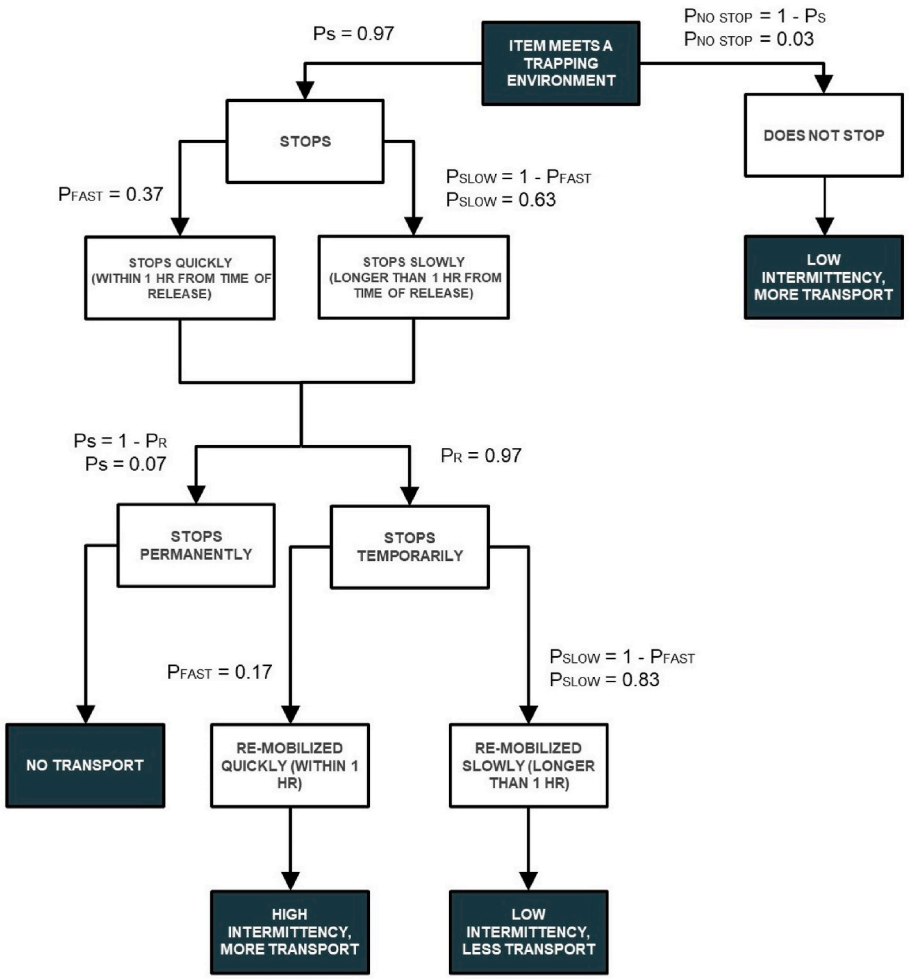

Fig. 3. Proposed conceptual model of a stopping and re-mobilization event of a floating riverine plastic item after it is released into a river system. Probabilities are based on the probabilities of stopping and re-mobilization from observations in the Saigon River, Vietnam (see Table 2).

the magnitude of the net transport. Items travelled significantly farther during spring tides than during neap tides (p-value = 0.029; 11.1 km day^{-1} and 7.0 km day^{-1} for spring and neap, respectively) (Appendix C and Appendix D.11C), demonstrating a dependence of total transport velocity on the prevailing tidal conditions, where spring tides contribute to greater current velocities. The ratio between the total and net velocities is significantly greater during spring tides than during neap tides (p = 0.005), indicating that spring tides lead to more total transport, while not necessarily increasing net transport or export.

We found a median residence time for all trajectories of 21 days for the 40 km system length. No significant differences were found for median residence times during ebb-flood and spring-neap tidal releases, with median values ranging between 20 and 24 days (Appendix C). While most trajectories had a residence time of less than 50 days (76%), 10% had residence times greater than 100 days. Outliers with high residence times values (in the order of several years, Appendix D.8B) result in a mean residence time of 202 days for all trajectories, with a large spread between values (±928 days, ranging from 1.5 to 6515 days) (Appendix C). Large residence times result from items being retrieved only a few tens of meters from their release locations.

3.4. The life cycle of a plastic item in the Saigon River in summary

Our results enable us to summarize the life cycle of a plastic item in the Saigon River. We report the median values, as well as the mean values in parenthesis, to illustrate the typical item trajectory. After one day in the system, an item will be retrieved 1.9 km (mean = 4.2 km) from where it was released, having travelled a total distance of 6.5 km (mean = 8.9 km). Depending on the state of the tide at its release, the item will be retrieved either downstream of its release point (62%) or upstream (37%). It will stop 0.12 times per hour (mean = 0.12), or 1.5 times throughout the tidal cycle, and the item will be stopped for 4.9 h (mean = 8.5 h). The item will come to a stop 1.1 h (mean = 2.5 h) after being released, and spend a little under half its time in the system stopped (stop time/total time: median = 0.51; mean = 0.49). The item will have a residence time of 21.2 days (mean = 202 days) in the 40 km river reach. The item will likely be retrieved within hyacinth patches (80%), and near the edge of the river (50%).

4. Discussion

4.1. Quantifying intermittency in plastic transport

Our case study demonstrates that river plastic transport can be intermittent, and that for tidally affected river reaches, the succession of transport and stopping phases can place at daily time-scales, as observed in the Saigon River. In addition to characterising transport intermittency and providing insights for the system we investigated, our approach also proposes novel metrics for quantifying this intermittency, such as the time to first stop and the ratio of time spent stopped and in motion. These could be used as a starting point for integrating the concept of intermittency and short-term retention in plastic transport studies and

models. In particular, we quantified for the first time the probabilities of an item stopping and becoming re-mobilized. In the Saigon River, the probability of stopping is larger than for re-mobilization, an indication that the conditions for trapping are more frequently met in the time and space domain considered than those for remobilization. This ultimately results in a net loss of items in the system during the study period.

Previous tracker experiments investigated plastic transfer dynamics over longer time-scales (e.g. weekly and monthly), and therefore had lower observation temporal frequency (~2 h in Tramoy et al. (2020a), ~ 3–4 h in Duncan et al. (2020)). As a consequence, such studies report stopping and re-mobilization metrics over the entire length of items trajectories, ranging from several days to weeks and months (21–23 days in Duncan et al. (2020) and median trajectory length of 22 days in Tramoy et al. (2020a)). These studies also define metrics related to transport and stopping by considering broader temporal windows than those investigated in our study. As such, these studies do not capture the fine-scale variability in plastic transport observed here. We found that in the Saigon River, 99% of items stop within 10 h of transport and 85% of items are re-mobilized within 10 h of stopping. The timescales at which items are stopped and re-mobilized, and the ratio of stopped to mobile items determines to a great extent how plastic items in a given river system are being transported and retained.

Despite different experimental set-ups and time-scales of interest, transport intermittency can be compared within and across systems by the metrics proposed in this paper, such as the ratio between stopping and transport time. To illustrate, ratio close to unity indicates equal time spent in motion and stopped, driven by high frequency shifts between transport and stopping phases. Large ratios ($>>1$) may indicate both low transport and low intermittency items are not easily re-mobilized and spend most of their time stopped. Low ratios ($<<1$) suggest a high transport mode dominated by continuous motion with low intermittency. Using GPS trackers, Tramoy et al. (2020a) found a high stopping to transport time ratio (8.5) for the sections of the Seine River not affected by bi-directional flow. This ratio was much lower (3) in the estuarine reaches, but still larger than what we found for the Saigon River (1:1–49 and 51% of stopping and transport time, respectively). Mani et al. (2023) found a ratio of 4:1 in the Chao Praya River. The Seine River has a greater tidal range than the Saigon, up to 7 m. The Chao Praya has a similar tidal range to the Saigon, approximately 2.5 m, but higher discharge of $\approx$2500 $m^3 s^{-1}$. Differences between these ratios can likely be linked to the different hydrological conditions and river characteristics, but are also due to the varying definitions for when an item is stopped. Mani et al. (2023), for example, considers that items stopped when their 60 min moving average speed was less than 0.1 m s^{-1}. Applied to the Saigon River, such a definition would have resulted in longer transport phases. Clear documentation of such definitions is key to ensure future plastic tracking studies are comparable.

4.2. Drivers of stopping and re-mobilization of plastic transport

Our study provides preliminary insights on the drivers of stopping and re-mobilization, suggesting that meanders, floating vegetation and presence of river infrastructure and vegetation that increase bank roughness all promote the trapping and stopping of items. However, more research on the morphological drivers of intermittency is necessary. In our study reach, we observed that downstream trajectories exhibited higher intermittency, with shorter travel distances than those upstream. We hypothesize that these differences can be explained by the higher trapping efficiency of downstream environments, which were less channelised, with more riparian vegetation and improvised embankments. Ledieu et al. (2022) found that stopping episodes occurred when items were trapped in riparian vegetation or stranded on riverbanks. For the Saigon River, trapping occurred primarily by in-stream vegetation; we found that items were frequently associated with water hyacinth patches (81% of items were retrieved within hyacinths, and retrievals overwhelmingly occurred when items had stopped). Only 6% of items (n = 10) were retrieved on riverbanks. Because hyacinth patches are free-floating and mainly accumulate on the river edges, they often formed a barrier between the item and the river bank, preventing items from becoming beached and increasing the likelihood of re-mobilization (Schreyers et al., 2021). In this way, the hyacinths in the Saigon River, covering up to 24% (Janssens et al., 2022), likely facilitates short-term trapping and re-mobilization at relatively higher rates.

4.3. Tidal dynamics influence both the magnitude and direction of net plastic transport

Our observations show that effect of tidal dynamics on the transport through and subsequent export of plastic items out of tidal river reaches and estuaries into the ocean are considerable, in line with the previous findings of Tramoy et al. (2020a,b); Ledieu et al. (2022); Mani et al. (2023). The median total travel distance per day was more than three times as high as their net travel distances. In the Saigon River, we found a ratio between net and total travelled distance per day of 1:2 and 1:3 (respectively for mean and median values), caused by bi-directional tidal transport. The ratio of net to total distance travelled was larger for the Seine River (1:4 and 1:5 for mean and median values) and lower for the Loire River (1:1.4 to 1:2.8 for mean and median values) (Tramoy et al., 2020a; Ledieu et al., 2022), indicating that the degree of tidal influence on distance travelled are system and location specific. The proportion of items ultimately travelling upstream vs. downstream is also sensitive to the direction of the tidal flow at the moment of release.

The tidal conditions at the moment of item release did not lead to significant differences in the metrics or probabilities of stopping, although higher probabilities of re-mobilization were found for spring and ebb release conditions than during flood and neap conditions. We did not monitor transport trajectories in a system without tidal influence however, stronger tidal conditions in spring than neap periods did not lead to significant differences in stopping or re-mobilization. Here, the combined effect of fluctuations in water level and flow velocities caused by the tides, as well as the presence of trapping environments can explain the succession of transport and stopping phases. Our results do emphasise the complex interactions between tidal dynamics, vegetation, local morphology, and hydro-meteorological factors that ultimately determine a trajectory's fate (van Calcar and van Emmerik, 2019; van Emmerik et al., 2019; Liro et al., 2020; Haberstroh et al., 2020; van Emmerik et al., 2022b).

4.4. Study limitations and future outlook

Transport, stopping, and re-mobilisation processes have been shown to depend on the physical properties of plastic items, hydrological conditions, and river morphology (Schwarz et al., 2019; Liro et al., 2020; van Emmerik et al., 2022b, 2023). Our experiments took place at the beginning of the rainy season, capturing the sub-daily to weekly effect tides on floating plastic transport. River discharge was on average 170 $m^3 s^{-1}$ during the study period, representing the typical range found in the Saigon River: −80 to 350 $m^3 s^{-1}$ (Camenen et al., 2021). However, the longer-term effect of seasonal variations in river discharge and its effects on plastic transport should not be overlooked. van Calcar and van Emmerik (2019) found that seasonal fluctuations of floating plastic transport can vary up to a factor of five in the Saigon River. During periods of higher freshwater discharge, tidal effects on the plastic transport may be attenuated, leading to higher plastic net travel distances and shorter residence times. While not the focus of this study, high discharge and flood events have been shown to rapidly mobilise plastics, although downstream transport may still be limited (van Emmerik et al., 2023; Hauk et al., 2023). We therefore recommend to conduct similar experiments to characterize plastic transport for a broad range of hydrological conditions using the proposed metrics.

Plastic transport dynamics depend on item characteristics, such as density, surface tension and size (Valero et al., 2022; Kuizenga et al.,

2022). In this study, we focus on positively buoyant items, but items with relative lower densities would likely exhibit different behaviour as well. In the Seine, Tramoy et al. (2020a) found a discrepancy in the behaviour of floating and half-submerged items that were released at the same time, attributing this to the effect of wind on the fully emerged particle trajectory. While we did not consider the effect of wind speed and wind direction, we hypothesize the wind can play a significant role in the lateral transport of buoyant plastic items towards the edges of the river channel, as substantiated by Browne et al. (2010); Sadri and Thompson (2014); van Emmerik et al. (2019).

Estimating river plastic transport as a function of discharge and plastic concentrations has been the basis for several plastic transport and emission models (Lebreton et al., 2017; Schmidt et al., 2017; Roebroek et al., 2022). However, Roebroek et al. (2022) showed that under non-flood conditions, discharge is a poor predictor for river plastic transport. We hypothesize this may be because such approaches neglect the intermittent nature of river plastic transport. Ultimately, it is necessary to broaden the current, transport-focused approach and include processes of stopping and retention in future plastic fate models. While most research on plastic transport in rivers focuses on plastic mobile phase and its drivers (van Emmerik et al., 2022a; Haberstroh et al., 2020), investigating stopping and re-mobilization processes could improve our current understanding of riverine plastic transport and retention dynamics. Additional Lagrangian observational data for different hydrological conditions are a starting point for a robust quantification of the governing factors. Flume studies could help quantify the role of morphological features such as channel sinuosity, bank structure and slope, vegetation cover, and estimate thresholds for stopping and re-mobilization under different hydrological conditions.

5. Conclusion

We used high frequency (10 s) Lagrangian observations of macroplastic trajectories in the Saigon River, Vietnam over the course of tidal cycles for a full month to provide data-driven insights into floating macroplastic behaviour under the influence of the tides. This data was used to explore the effect of the tide on the transport, trapping, re-mobilisation of macroplastic items in the Saigon River on short (daily - weekly) timescales.

Our observations showed that items stop just a few hours after being released, and spent almost half their time in the system stopped, but were readily re-mobilized. River morphology, and the presence of vegetation and infrastructure played a key role in trapping items, leading to a median retention time of 21 days. The probability of re-mobilization increases from neap to spring (neap: 0.86, spring: 1.00), suggesting that the stopping and successive re-mobilisation of an item is also influenced by tidal dynamics. Tidal dynamics further led to continuous back-and-forth transport, where total distances travelled per day were three times greater than the net distances travelled (median total velocity: 8.9 km d^{-1}; median net velocity: 2.0 km d^{-1} in the upstream direction and 1.6 km d^{-1} in the downstream direction), and total distance travelled increases from spring to neap. The tide also plays a key role in determining the ultimate direction of transport. Items released during flood tide were more likely to be retrieved upstream of their release point and items released during ebb were more likely to be retrieved downstream. In total, 81% of all retrieved items were trapped within water hyacinths.

We highlight the need for additional measurements in tidal reaches over a range of timescales and hydrological conditions in order to be able to extrapolate mean estuary behaviour, and subsequently estimate plastic export. We also encourage future research to build on the results presented here to improve our fundamental understanding of the processes behind stopping and re-mobilization for different plastic characteristics and environments.

With these results, we provide data-driven insights into macroplastic transport and trapping dynamics in a tropical tidal river at sub-daily timescales. Our findings highlight the need for a complete understanding of the full spectrum of macroplastic behaviour, including transport, stopping and remobilization, the interaction between plastic items and their environment, as well as tidal and hydrological conditions. Understanding these processes are crucial for the development of effective modelling, monitoring, and intervention strategies.

Funding

The work of TvE was supported by the Veni Research Program, the River Plastic Monitoring Project with project number 18211, which was (partly) financed by the Dutch Research Council (NWO).

CRediT authorship contribution statement

R.A. Lotcheris: Conceptualization, Data curation, Formal analysis, Investigation, Methodology, Resources, Software, Validation, Visualization, Writing – original draft, Writing – review & editing. **L.J. Schreyers:** Conceptualization, Investigation, Methodology, Writing – original draft, Writing – review & editing. **T.K.L. Bui:** Investigation, Project administration, Writing – review & editing. **K.V.L. Thi:** Investigation, Project administration, Writing – review & editing. **H.-Q. Nguyen:** Writing – review & editing. **B. Vermeulen:** Writing – review & editing. **T.H.M. van Emmerik:** Conceptualization, Funding acquisition, Investigation, Methodology, Project administration, Resources, Supervision, Writing – original draft, Writing – review & editing.

Declaration of competing interest

The authors declare that they have no known competing financial interests or personal relationships that could have appeared to influence the work reported in this paper.

Data availability

Data will be made available on request.

Appendix A. Extended methods

A total of 15 trackers was used (https://www.libitechnologies.com/LT21.html), of which 6 were lost very close to the start of the fieldwork campaign; the remaining 9 were used for the duration of the project, during which no additional losses occurred. Each tracker was placed in a reusable zip-lock bag along with a note explaining the nature and purpose of the experiment, in the event someone were to find and open the tracker container. The zip-lock bag was then taped inside an expanded polystyrene (EPS) box (20 × 15 × 15 cm), which was sealed with duct tape and put in a plastic bag to deter people from investigating its contents. This also ensured the tracker set-up was waterproof. It should be noted that the items in this study were consistently released from the centre of bridges in the middle of the channel, and thus began their transport as far away as practically possible from potential trapping environments near the river's edge. This means that the trajectories likely represent near-maximum transport capacity of the Saigon River.

Appendix A.1. Pre-processing

We defined three cases of gaps in the data. This was done by looking at how long the tracker remained within a certain area. The tracker signal, especially when the tracker was stopped in or around infrastructure and vegetation, was often sporadic, with bigger errors than when in motion. To account for this, the maximum diameter in which a tracker could be considered stopped was taken to be 30 m, which was estimated by measuring the scatter around several stopped points. The lowest flow measured across all bridges was 0.05 m s^{-1}. At this speed, a tracker would travel 45 m in 15 min. Based on this, a tracker was deemed to have stopped if it remained within an area with a 30 m diameter for at least 30 min. Stop detection was done using the Moving Pandas package (Version 0.11) by Graser (2019), used for network and movement data analysis. The three cases are detailed below, were, Δt represents the time interval between two successive points.

Case 1. The tracker has stopped, defined as $\Delta t > 1800$ s within a diameter < 30 m.

Case 2. There is a gap in the data, but the gap is short enough that we can reasonably assume the trajectory of the tracker. This case was defined as $1800 \text{ s} < \Delta t < 3600$ s with a diameter > 30 m. These points were still included in the analysis.

Case 3. There is a gap in the data, but the gap is so large that we cannot reasonably assume the behaviour or trajectory of the tracker. This case was defined as $\Delta t > 3600$ s with a diameter > 30 m. The times during which the position of the tracker could not be determined were discarded as missing data.

Before assigning stops and removing the missing periods of data, the average maximum Δt of all trajectories was 64,104 s, or 17 h. After accounting for periods where a tracker was stopped and discarding the periods where Δt exceeded 1 h, the average maximum Δt was 50 min, and the average was 10 s.

This stop detection strategy was applied to each trajectory to identify the number of stops, start time, end time, location, and respective duration of each stop, as well as remove missing data. On average, trajectories had 10 intervals where $\Delta t > 1$ h, thus falling into Case 3. Overall however, these accounted for just 1.1% of the total trajectory data points. If long intervals were at the end of a trajectory, this would in some cases reduce the length of certain trajectories fairly significantly. This, as well as the fact that some trackers remained in the system for longer periods of time, led to some discrepancies in the trajectory lengths.

Appendix A.2. Calculating transport and stopping metrics

The morphology of the river provides two different travel paths an item might take. An item could either travel around the meander, or take a shortcut through an artificial channel to join up with the meander downstream (see Fig. 1). The path taken by each trajectory was verified before calculating net distance. In the calculation of net and total distance, the points were snapped to a line in the centre of the river channel. This means the lateral movement of an item across a channel was not captured. Given the large distances however, this represents just a small fraction of an item's transport.

Appendix A.3. Probabilities of stopping

The probability of stopping (P_S) and re-mobilization (P_R) for all trajectories over their full lengths are defined simply as:

$$p_s = \frac{n_{stop} >= 1}{n} \tag{A.1}$$

$$p_s = \frac{n_{stop} >= 2}{n} \tag{A.2}$$

The timescale associated with these probabilities is the average trajectory length, 2 days and 12 h. The probability of re-mobilization here is the probability of stopping twice, and does not capture the items that stopped just once (n = 7), re-mobilized, and did not stop again. To identify those, the end time of item trajectories with just one stop were compared to the end times of the stop. If they were the same, it was assumed the item stopped once and never re-mobilized (n = 2). If they were different, it was assumed the item was re-mobilized (n = 2). For three of these, the trajectories had missing data at the end and were removed from the statistical calculation. For the remainder, the statistics were adjusted accordingly.

An item was defined as having left the system boundaries when it was retrieved past the upstream boundary, or when, due to the risk of being lost to the confluence and no longer being retrievable, it had to be collected near the downstream boundary. The probability of leaving the system is given for the entire trajectory length, and the timescale associated with this probability is therefore the average trajectory length, 2 days and 12 h. System boundaries were defined as 5 km upstream of the most upstream bridge, and at the confluence of the Saigon and Dong Nai Rivers (Fig. 1.

Appendix A.4. Retrieval sites

A nested framework was used to categorise the locations where items were found. First, the cross-sectional location within the river channel is established. These were separated into.

1. Near/at the channel edge; 2. Near/at the channel centre;
3. In a canal.

The second level of categorisation was the mode of trapping the item was associated with. This was either.

1. In infrastructure; 2. In riparian vegetation;
3. None (free-floating).

Infrastructure included any anthropogenic structures such as boats, docks, groynes, buoys or pontoons. The third and final level of categorisation was whether or not the item was associated with water hyacinths.

Appendix B. Water level and tidal analysis

The water level (WL) was calculated from the difference in water pressure between pressure sensors at the water surface and submerged near the riverbed according to Equation B.1

$$WL = \frac{p_{driver} - p_{baro}}{p^* g} \tag{B.1}$$

Where ρ is the density of water, here assumed to be estimated to be 1 g cm^{-3}, g is gravitational acceleration, and p_{diver} and p_{baro} are the pressures measured by the submerged and un-submerged divers, respectively.

The observed water level data was then used in the T _Tide MATLAB Toolbox written by Pawlowicz et al. (2002) to model the full water level timeseries. The observed water level, predicted water level, and the difference are shown in Figure B4. Sections of the observed water level data were truncated, caused by the water level dropping below the submerged water pressure logger. Because water levels dropped lower during springs tides, this contributed to a greater difference between the observed and modelled water level in these periods. Further differences might be explained by a delayed effect of precipitation on water level, higher river discharge, or strong wind currents. These may non-linearly affect the tidal analysis results as non-tidal influences on water level in this time period. Nonetheless, T Tide was able to accurately represent the observed water levels, and estimated 95% of the total water level observational signal to be explained by the tides.

The T Tide model fit 29 constituents, and deemed 19 of these to be significant. The results of the T Tide model indicated that the M2, K2, O1, S2, and N2, are the constituents with the highest amplitudes. Higher frequency, compound tides are also relevant. These tides arise from the interactions between the harmonic constituents, and their interaction with the channel morphology as the tidal wave travels further up the river.

The modelled tidal data was used to infer periods of flood, ebb, and slack water based on when high and low water occurred. Slack water was defined as 30 min either side of the local maximum and minimum water level. The period of rising and falling tide between these subsequent points was then defined as flood and ebb, respectively. Often, despite for example water level being at a maximum, current velocities have not yet slowed down and are still in the flood phase. Likewise, even though water level might be at a minimum, current velocities might still be in ebb. It was necessary to account for this phase shift when defining the start and end of flood, ebb, and slack periods.

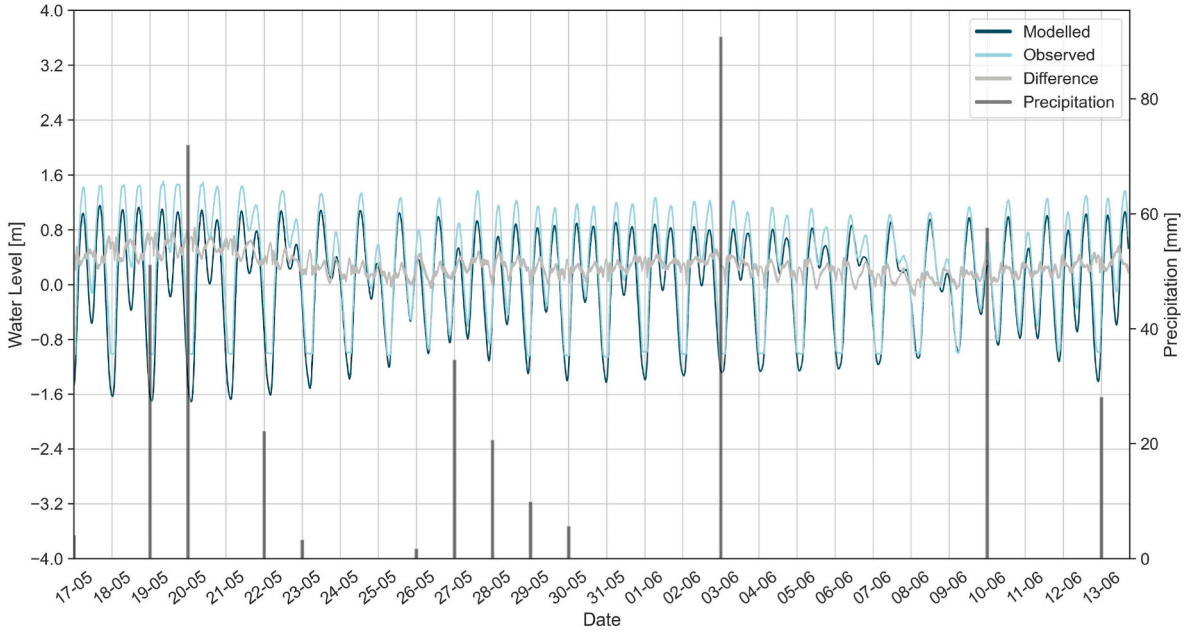

Fig. B.4. The truncated observed water level (light blue) is shown behind the modelled water level (dark blue). The difference between the two is given in grey. Measured precipitation in Ho Chi Minh City for the study period is shown by the bars.

Continuous discharge and water level measurements were taken for four days in the week leading up to the fieldwork period. Figure B.5 shows the water level and discharge for this period. The phase shift between the time when water level is at its maximum and discharge is close to 0 is evident. To calculate this shift, the average time difference between these points was calculated for 5 high water periods in the time series. It should be noted here that the current velocity measurements were not done at the release location, but 15 km downstream. They were also carried out for just three days, and we therefore assume a phase shift that is constant in time which may not be the case. These measurements were conducted in early May 2022 (Schreyers et al., 2022; in preparation). Nonetheless, this revealed a mean phase shift of 01:36 h, which was included in the start and end times of the flood and ebb periods.

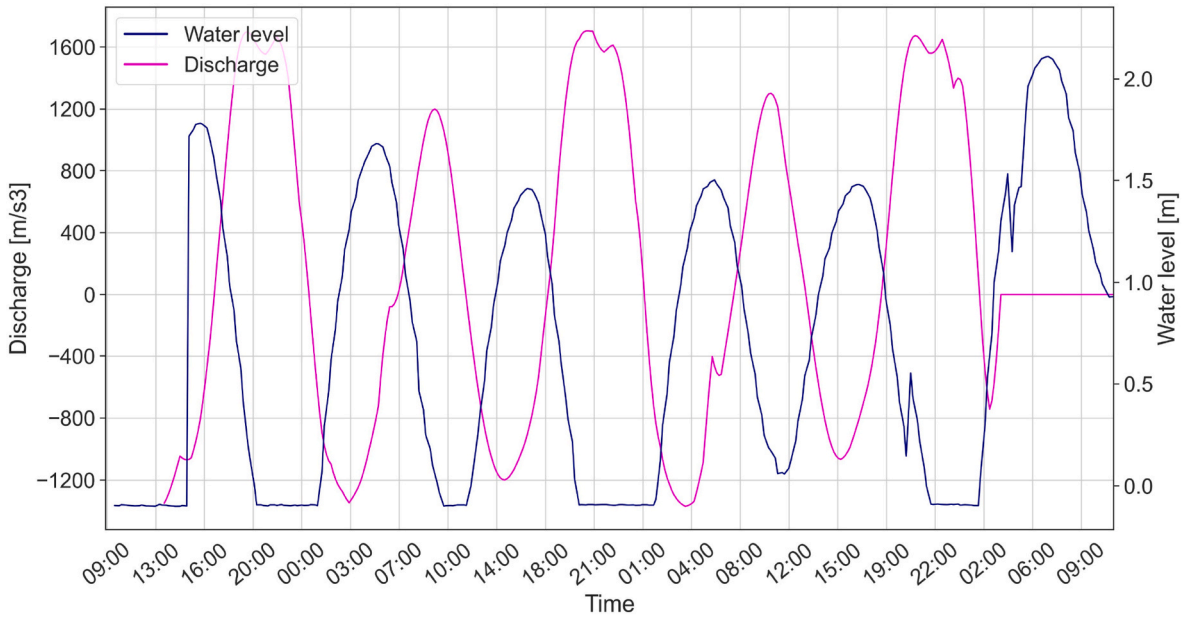

Fig. B.5. Water level and discharge measured in from 09:00 May 1st to 09:00 May 4th by (Schreyers et al., 2023). The time difference between maximum water level and 0 discharge was used to estimate the phase shift between high water and slack tides.

Appendix C. Summary statistics

Table C.3
Summary statistics for all metrics of all trajectories and for trajectories grouped by the tidal conditions of release.

Variable			Tide phase		Tide state	
	Measure	Total	Spring	Neap	Flood	Ebb
Net velocity downstream [km day^{-1}]	Mean	4.199	4.182	4.214	4.325	4.086
	Std	5.405	4.068	6.603	4.945	5.920
	Median	2.029	3.400	1.752	1.984	2.075
	Max.	26.31	16.84	26.31	16.84	26.31
	Min.	6.139	0.215	6.139	0.463	6.139
Net velocity upstream [km day^{-1}]	Mean	3.958	2.033	5.291	4.737	1.312
	Std	4.913	3.196	5.544	5.322	1.463
	Median	1.636	0.818	4.014	1.640	0.819
	Max.	16.74	10.12	16.74	16.74	3.352
	Min.	13.57	0.014	0.086	0.226	0.014
Total velocity [km day^{-1}]	Mean	8.920	11.10	7.030	8.356	9.715
	Std	7.640	8.900	5.860	6.792	8.794
	Median	6.510	8.900	5.850	6.485	7.613
	Max.	33.70	33.70	26.30	31.70	33.72
	Min.	0.297	0.297	0.548	0.297	0.827
Stop time/total time [-]	Mean	0.487	0.498	0.475	0.511	0.450
	Std	0.272	0.252	0.297	0.294	0.235
	Median	0.512	0.525	0.489	0.535	0.489
	Max.	0.990	0.930	0.990	0.990	0.838
	Min.	0.000	0.094	0.000	0.000	0.000
Stops per hour [-]	Mean	0.124	0.122	0.124	0.129	0.116
	Std	0.092	0.051	0.118	0.110	0.060
	Median	0.121	0.133	0.114	0.121	0.117
	Max.	0.600	0.267	0.600	0.600	0.267
	Min.	0.000	0.040	0.000	0.000	0.000
Mean stop time [hours]	Mean	8.48	6.35	10.3	7.80	9.44
	Std	9.88	7.49	11.4	8.30	11.9
	Median	4.85	3.90	6.37	5.29	3.72
	Max.	40.0	36.2	40.0	36.2	39.9
	Min.	0.00	0.58	0.00	0.00	0.00
Time to first stop [hours]	Mean	2.530	2.700	2.370	2.42	1.83
	Std	4.070	3.460	4.640	5.24	2.35
	Median	1.120	1.080	1.130	1.00	1.00
	Max.	25.00	15.20	25.00	25.0	8.00
	Min.	0.050	0.051	0.050	0.00	0.37
Residence time [days]	Mean	202.0	145.0	252.0	34.34	440.0
	Std	928.0	562.0	1166	41.80	1426
	Median	21.18	24.39	20.16	21.18	21.39
	Max.	6516	2947	6515	177.3	6516
	Min.	1.518	2.376	1.518	1.876	1.518

Appendix D. Supplementary figures

Appendix D.1. Simple conceptual summary model of transport pathways of an item in the Siagon River, Vietnam

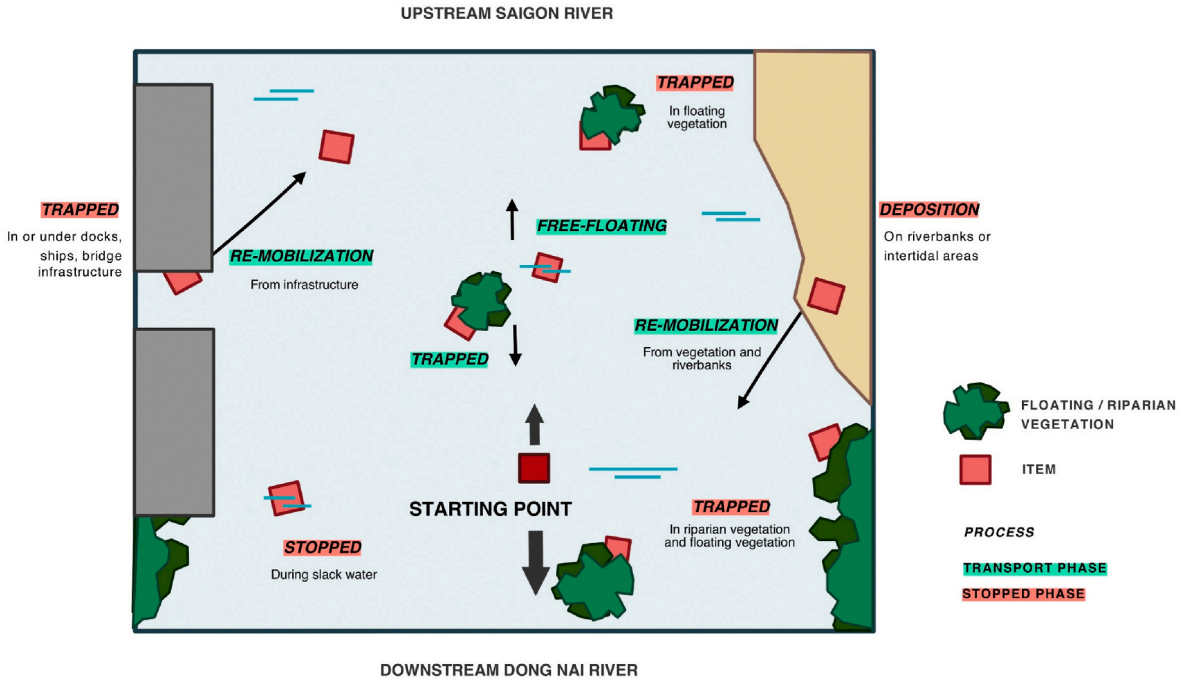

Fig. D.6. Simple conceptual model of the transport pathways of a plastic item. Two transport modes are labelled according to a colour key: transport in green and stopping in red. Different processes or mechanisms of stopping and transport are labelled. These mechanisms include trapping in infrastructure or vegetation and deposition on riverbanks. An item can also be re-mobilized from any these environments. For transport phases, possible directions of transport are given by arrows. In a tidal system, transport can occur in both the up- and downstream directions and stops can be caused by low/no flow during slack water. Larger arrows are scaled according to the proportion of items that were transport up or downstream. Both modes can occur while an item is associated with floating vegetation.

Appendix D.2. Fitting the exponential function for the time to first stop

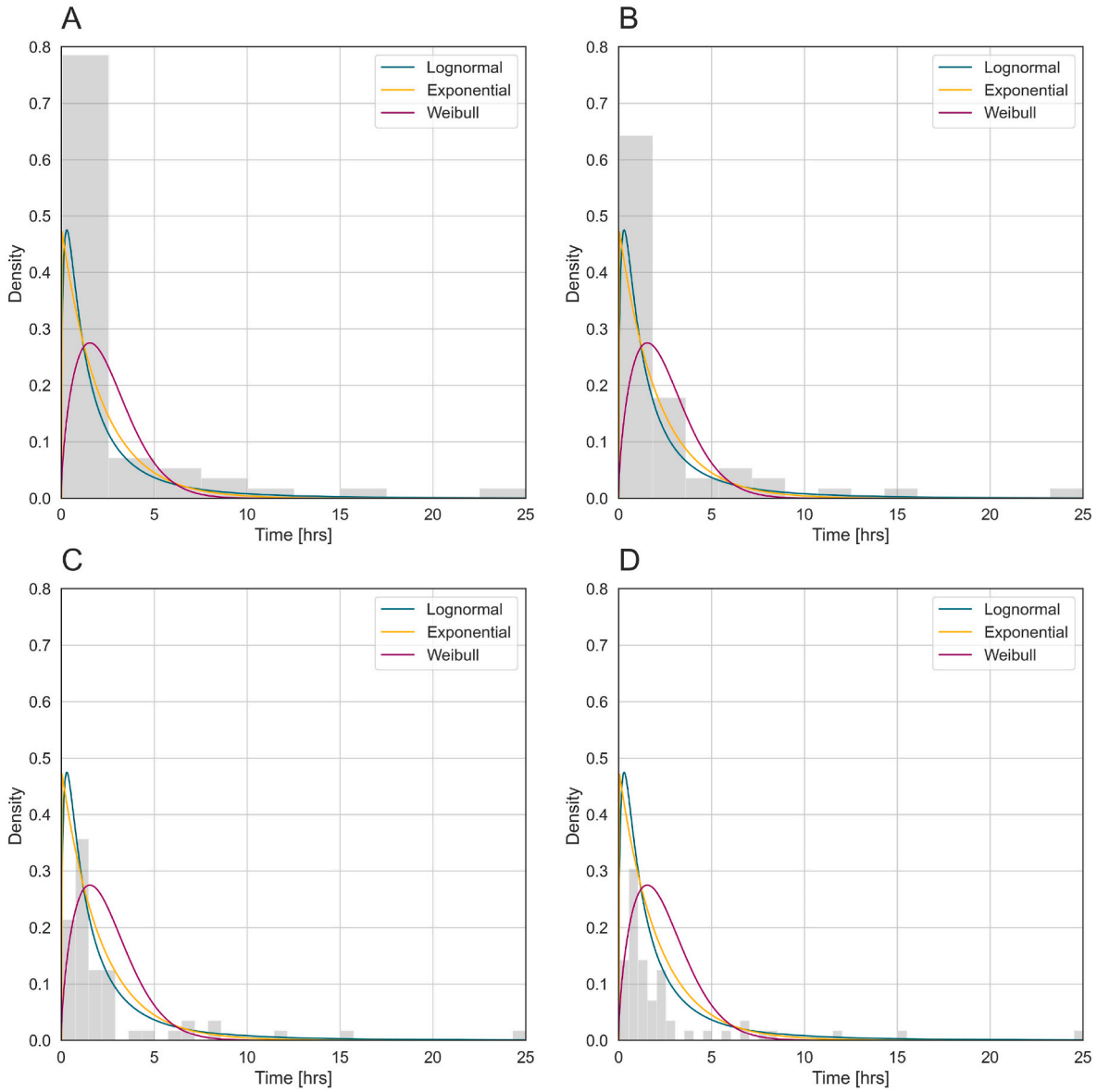

Fig. D.7. Histograms of the time to first stop for number of bins n = 10 (A), n = 15 (B), n = 35 (C), and n = 50 (D). Log-normal, exponential, and Weibull distributions are fit. A bin size of 15 was selected based on a smooth fit and accurate representation of the underlying distribution. An exponential function provided the best fit, confirmed by AIC and BIC values.

Appendix D.3. Probability density function of the time to first stop and residence times

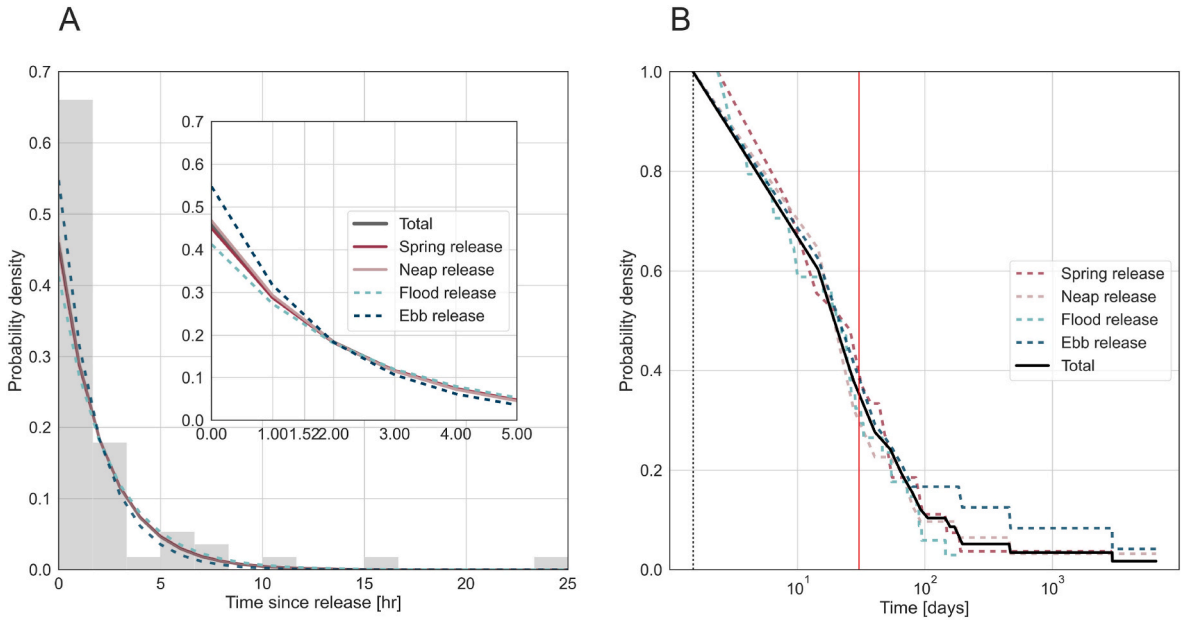

Fig. D.8. (A) Fitted probability density function of distribution of the time to first stop. Release conditions were either during spring (n = 27) or neap (n = 31), and during flood (n = 34) or ebb (n = 24). The distribution can be well represented with an exponential distribution function. The probability distributions under different tidal release conditions are given in the blue and red lines. The histogram of the observed count density for all trajectories is also shown. The inset graph shows in more detail the probability distribution of the time to first stop for the first 5 h after release. (B) Probability density of residence times. Note the logarithmic scale, an indication of the significant spread in residence time; the distribution takes the form of an exponential. The red line indicates the 30-day residence time, and the dashed line indicates the minimum time required to leave system (1.52 days). Most particles have a 40% probability of exceeding 30 days in the system.

Appendix D.4. Ratio between the total distance travelled per day and the net distance travelled per day

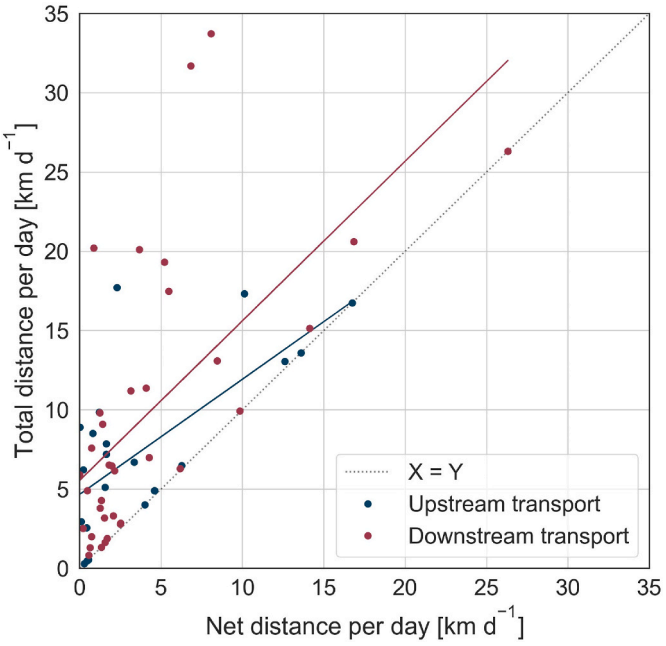

Fig. D.9. The relationship between the net and total distances for items with a net upstream transport direction in blue and a net downstream transport direction in red. Lines of best fit are shown for both in corresponding colors with p = 0.012 for upstream transport, and p = 1.43e−5 for downstream transport. While there was a significant, positive correlation between the two, the distribution is chaotic and a linear relation is not immediately clear.

Appendix D.5. Statistical distribution of the net and total distance travelled

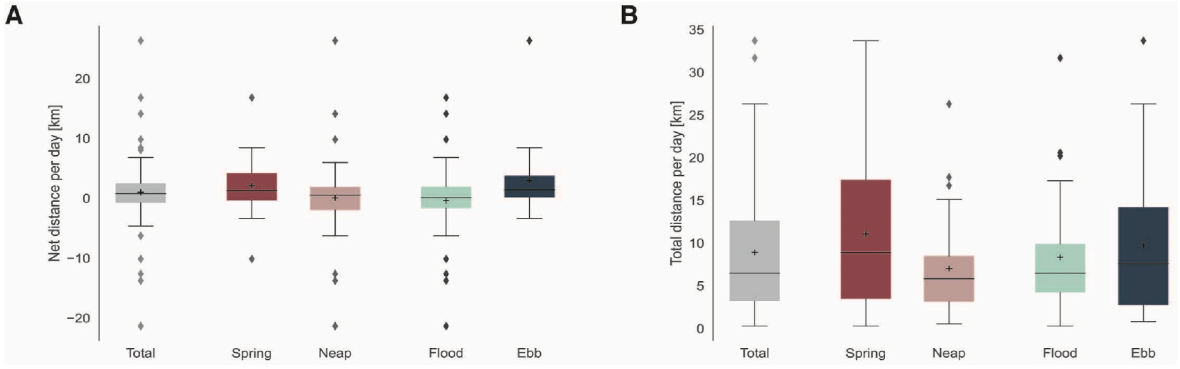

Fig. D.10. Box plots showing the distribution of the net (A) and total (B) distances travelled per day of all trajectories and of trajectories under different release conditions. Release conditions were either during spring (n = 27) or neap (n = 31), and during flood (n = 34) or ebb (n = 24). Figure A shows relatively low variability between the different tidal release conditions for the net distance, whereas figure B shows much more difference between them for the total transport. The magnitude of total transport is also larger than that of net transport.

Appendix D.6. Cumulative distribution of the distances travelled

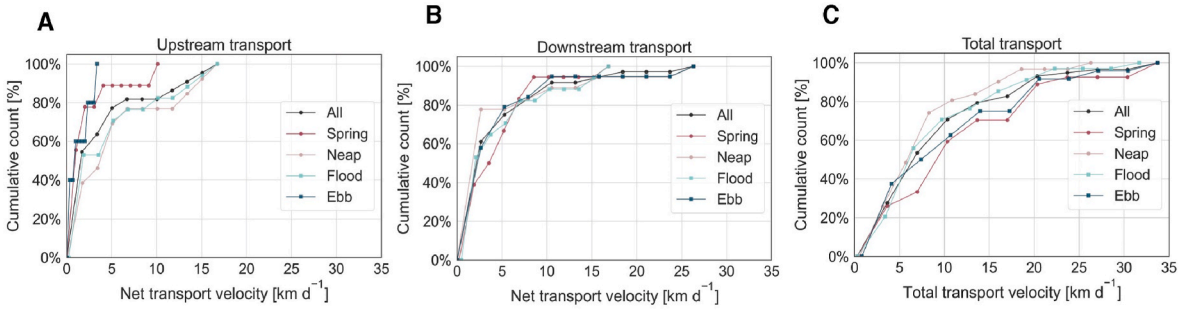

Fig. D.11. Cumulative distribution of the net distances travelled in the upstream direction (A) and downstream direction (B) and total distances travelled (C).

Appendix D.7. Summary of Mann-Whitney U tests

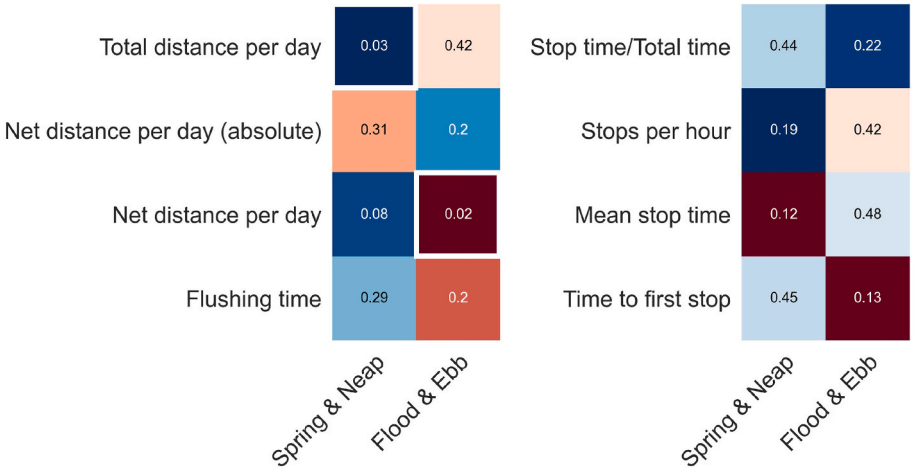

Fig. D.12. The difference in the metrics of transport and trapping are compared under different tidal release conditions using a one-sided Mann-Whitney *U* test. The tidal variables compared are given on the x-axis. A red color indicates the first variable was smaller than the second, and a blue color indicates the first variable was larger than the second. The darkness of the color indicates the magnitude of difference, with darker colors meaning the two variables are more different. The p-values are reported in the grid cells, and significant results are highlighted.

Appendix D.8. Trajectory classification

Figure D.13presents several example trajectories in different categories, illustrating both the variability in potential transport patterns and the typical paths a trajectory might take.

Trajectories were classified according to their shared transport characteristics (Figure D.13). They were deemed short if the distance between their most upstream and most downstream points was less than 5 km, long if it was between 5 and 15 km, and very long if it was greater than 15 km. Trajectories were also given a secondary classification based on whether the item was only transported downstream of the release point, upstream of the release point, or whether the item travelled in both the up- and downstream sections with respect to their release point. Most trajectories were short (< 5 km) ($n = 27$), and most travelled both up and downstream ($n = 31$). Out of 58 items, 38% had a net upstream transport direction upstream ($n = 22$) and 62% had a net downstream transport direction ($n = 36$).

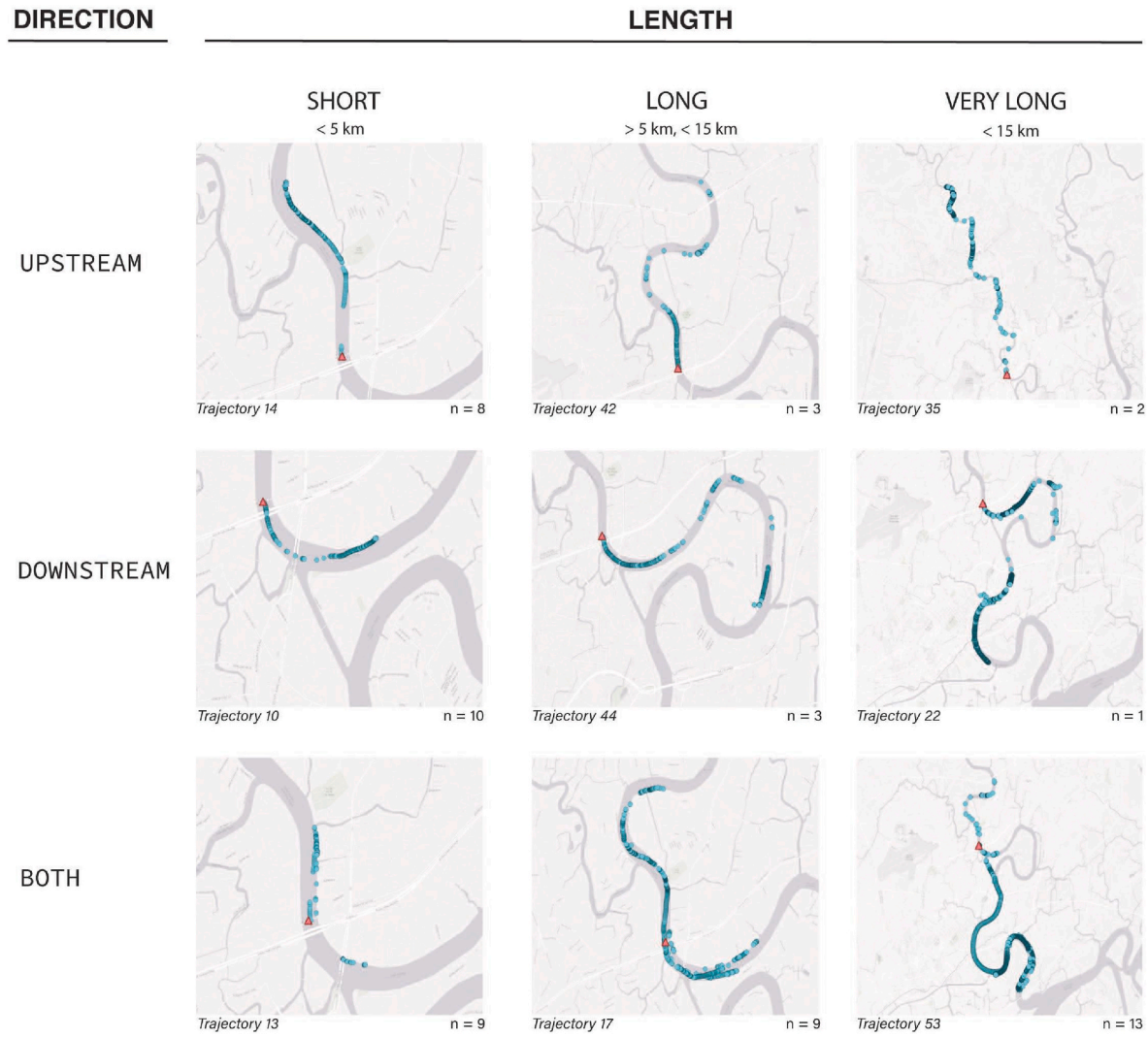

Fig. D.13. The general classification of trajectories, including an example for each trajectory class and the number of trajectories contained within that class. The release location is given in red. Darkened points indicate overlapping transport. Trajectories were could be classified into several broad groups. Trajectories could either be short (<5 km), long (between 5 km and 15 km), or very long (>15 km), measured from their most upstream point to their most downstream point (top to bottom). They were also classified as having travelled only upstream form the release location, given here in red, only downstream of their release location, or in both the upstream and downstream areas. Most trajectories were short (< 5 km) and most travelled in both areas. Combining both groupings, the highest count in a single group was trajectories that were very long and travelled in both regions.

References

Acha, M., Mianzan, H., Iribarne, O., Gagliardini, D., Lasta, C., Daleo, P., 2003. The role of the Rıo de la Plata bottom salinity front in accumulating debris. Mar. Pollut. Bull. 46, 197–202. https://doi.org/10.1016/S0025326X(02)00356-9.

Blondel, E., Buschman, F.A., 2022. Vertical and horizontal plastic litter distribution in a bend of a tidal river. Front. Environ. Sci. 10 https://doi.org/10.3389/fenvs.2022.861457.

Browne, M.A., Galloway, T.S., Thompson, R.C., 2010. Spatial patterns of plastic debris along estuarine shorelines. Environmental Science &amp$\mathsemicolon$ Technology 44, 3404–3409. https://doi.org/10.1021/es903784e publisher: American Chemical Society (ACS).

Valle-Levinson, A., 2010. Contemporary Issues in Estuarine Physics. Cambridge University Press, Cambridge.

van Calcar, C.J., van Emmerik, T., 2019. Abundance of plastic debris across European and Asian rivers. Environmental Research Letters 14, 124051. https://doi.org/10.1088/1748-9326/ab5468 (publisher: IOP Publishing).

Camenen, B., Gratiot, N., Cohard, J.A., Gard, F., Tran, V.Q., Nguyen, A.T., Dramais, G., Emmerik, T.v., Némery, J., 2021. Monitoring discharge in a tidal river using water level observations: application to the Saigon River, Vietnam. Science of The Total Environment 761, 143195. https://doi.org/10.1016/j.scitotenv.2020.143195 (publisher: Elsevier BV).

Chan, H.H., Not, C., 2023. Variations in the spatial distribution of expanded polystyrene marine debris: are asian's coastlines more affected? Environmental Advances 11, 100342. https://doi.org/10.1016/j.envadv.2023.100342. URL: https://www.sciencedirect.com/science/article/pii/S2666765723000029.

Duncan, E.M., Davies, A., Brooks, A., Chowdhury, G.W., Godley, B.J., Jambeck, J., Maddalene, T., Napper, I., Nelms, S.E., Rackstraw, C., Koldewey, H., 2020. Message in a bottle: open source technology to track the movement of plastic pollution. PLOS ONE 15, e0242459. https://doi.org/10.1371/journal.pone.0242459 publisher: Public Library of Science (PLoS).

van Emmerik, T., van Klaveren, J., Meijer, L.J.J., Krooshof, J.W., Palmos, D.A.A., Tanchuling, M.A., 2020. Manila River mouths act as temporary sinks for macroplastic pollution. Frontiers in Marine Science 7. URL: https://www.frontiersin.org/article/10.3389/fmars.2020.545812.

van Emmerik, T., de Lange, S., Frings, R., Schreyers, L., Aalderink, H., Leusink, J., Begemann, F., Hamers, E., Hauk, R., Janssens, N., Jansson, P., Joosse, N., Kelder, D., van der Kuijl, T., Lotcheris, R., Löhr, A., Mellink, Y., Pinto, R., Tasseron, P., Vos, V., Vriend, P., 2022a. Hydrology as a driver of floating river plastic transport. Earth's Future 10. https://doi.org/10.1029/2022ef002811.

van Emmerik, T., Mellink, Y., Hauk, R., Waldschlager, K., Schreyers, L., 2022b. Rivers as plastic reservoirs. Frontiers in Water 3. https://doi.org/10.3389/frwa.2021.786936 (publisher: Frontiers Media SA).

van Emmerik, T., Schwarz, A., 2020. Plastic debris in rivers. WIREs Water 7. https://doi.org/10.1002/wat2.1398 (publisher: Wiley).

van Emmerik, T., Strady, E., Kieu-Le, T.C., Nguyen, L., Gratiot, N., 2019. Seasonality of riverine macroplastic transport. Scientific Reports 9. https://doi.org/10.1038/s41598-019-50096-1 (publisher: Springer Science and Business Media LLC).

van Emmerik, T.H.M., Frings, R.M., Schreyers, L.J., Hauk, R., de Lange, S.I., Mellink, Y.A. M., 2023. River plastic transport and deposition amplified by extreme flood. Nature Water 1, 514–522. https://doi.org/10.1038/s44221-02300092-7.

Graser, A., 2019. MovingPandas: efficient structures for movement data in Python. GI Forum 1, 54–68. https://doi.org/10.1553/giscience2019.01.s54 (publisher: Osterreichische Akademie der Wissenschaften).

Haberstroh, C.J., Arias, M.E., Yin, Z., Wang, M.C., 2020. Effects of hydrodynamics on the cross-sectional distribution and transport of plastic in an urban coastal river. Water Environment Research 93, 186–200. https://doi.org/10.1002/wer.1386 (publisher: Wiley).

Hauk, R., van Emmerik, T.H.M., van der Ploeg, M., de Winter, W., Boonstra, M., Löhr, A. J., Teuling, A.J., 2023. Macroplastic deposition and flushing in the meuse river following the july 2021 european floods. Environmental Research Letters 18, 124025. https://doi.org/10.1088/1748-9326/ad0768.

Jambeck, J.R., Geyer, R., Wilcox, C., Siegler, T.R., Perryman, M., Andrady, A., Narayan, R., Law, K.L., 2015. Plastic waste inputs from land into the ocean. Science 347, 768–771. https://doi.org/10.1126/science.1260352 publisher: American Association for the Advancement of Science (AAAS).

Janssens, N., Schreyers, L., Biermann, L., van der Ploeg, M., Bui, T.K.L., van Emmerik, T., 2022. Rivers running green: water hyacinth invasion monitored from space. Environmental Research Letters 17, 044069. https://doi.org/10.1088/1748-9326/ac52ca.

Kuizenga, B., van Emmerik, T., Waldschlager, K., Kooi, M., 2022. Will it float? rising and settling velocities of common macroplastic foils. ACS Es&t Water 2, 975–981.

Lahens, L., Strady, E., Kieu-Le, T.C., Dris, R., Boukerma, K., Rinnert, E., Gasperi, J., Tassin, B., 2018. Macroplastic and microplastic contamination assessment of a tropical river (Saigon River, Vietnam) transversed by a developing megacity. Environmental Pollution 236, 661–671. https://doi.org/10.1016/j.envpol.2018.02.005 (publisher: Elsevier BV).

Lebreton, L.C.M., Zwet, J.v.d., Damsteeg, J.W., Slat, B., Andrady, A., Reisser, J., 2017. River plastic emissions to the world's oceans. Nature Communications 8. https://doi.org/10.1038/ncomms15611 (publisher: Springer Science and Business Media LLC).

Ledieu, L., Tramoy, R., Mabilais, D., Ricordel, S., Verdier, L., Tassin, B., Gasperi, J., 2022. Macroplastic transfer dynamics in the Loire estuary: similarities and specificities with macrotidal estuaries. Marine Pollution Bulletin 182, 114019. https://doi.org/10.1016/j.marpolbul.2022.114019 (publisher: Elsevier BV).

Liro, M., Emmerik, T.v., Wyzga, B., Liro, J., Mikuś, P., 2020. Macroplastic storage and remobilization in rivers. Water 12, 2055. https://doi.org/10.3390/w12072055 (publisher: MDPI AG).

Mani, T., Hawangchu, Y., Khamdahsag, P., Lohwacharin, J., Phihusut, D., Arsiranant, I., Junchompoo, C., Piemjaiswang, R., 2023. Gaining new insights into macroplastic transport 'hotlines' and fine-scale retentionremobilisation using small floating high-resolution satellite drifters in the chao phraya river estuary of bangkok. Environmental Pollution 320, 121124. https://doi.org/10.1016/j.envpol.2023.121124.

Meijer, L.J.J., Emmerik, T.v., Ent, R.v.d., Schmidt, C., Lebreton, L., 2021. More than 1000 rivers account for 80% of global riverine plastic emissions into the ocean. Science Advances 7. https://doi.org/10.1126/sciadv.aaz5803 publisher: American Association for the Advancement of Science (AAAS).

Monsen, N.E., Cloern, J.E., Lucas, L.V., Monismith, S.G., 2002. A comment on the use of flushing time, residence time, and age as transport time scales. Limnology and Oceanography 47, 1545–1553. https://doi.org/10.4319/lo.2002.47.5.1545 (publisher: Wiley).

Nakayama, T., Osako, M., 2023. The flux and fate of plastic in the world's major rivers: modelling spatial and temporal variability. Global and Planetary Change 221, 104037. https://doi.org/10.1016/j.gloplacha.2023.104037.

Nguyen, A.T., Némery, J., Gratiot, N., Garnier, J., Dao, T.S., Thieu, V., Laruelle, G.G., 2021. Biogeochemical functioning of an urbanized tropical estuary: implementing the generic C-GEM (reactive transport) model. Science of The Total Environment 784, 147261. https://doi.org/10.1016/j.scitotenv.2021.147261 (publisher: Elsevier BV).

Pawlowicz, R., Beardsley, B., Lentz, S., 2002. Classical tidal harmonic analysis including error estimates in MATLAB using T tide. Computers &amp$\mathsemicolon$ Geosciences 28, 929–937. https://doi.org/10.1016/s00983004(02)00013-4 (publisher: Elsevier BV).

Roebroek, C.T.J., Harrigan, S., Emmerik, T.H.M.v., Baugh, C., Eilander, D., Prudhomme, C., Pappenberger, F., 2021. Plastic in global rivers: are floods making it worse? Environmental Research Letters 16, 025003. https://doi.org/10.1088/1748-9326/abd5df (publisher: IOP Publishing).

Roebroek, C.T.J., Laufkötter, C., González-Fernández, D., Emmerik, T.v., 2022. The quest for the missing plastics: large uncertainties in river plastic export into the sea. Environmental Pollution 312, 119948. https://doi.org/10.1016/j.envpol.2022.119948 (publisher: Elsevier BV).

Sadri, S.S., Thompson, R.C., 2014. On the quantity and composition of floating plastic debris entering and leaving the Tamar Estuary, Southwest England. Marine Pollution Bulletin 81, 55–60. https://doi.org/10.1016/j.marpolbul.2014.02.020 (publisher: Elsevier BV).

Savenije, 2006. Salinity and Tides in Alluvial Estuaries. Environmental Science &amp$\mathsemicolon$ Technology.

Schmidt, C., Krauth, T., Wagner, S., 2017. Export of plastic debris by rivers into the sea. Environmental Science &amp$\mathsemicolon$ Technology 51, 12246–12253. https://doi.org/10.1021/acs.est.7b02368 publisher: American Chemical Society (ACS).

Schreyers, L., van Emmerik, T., Nguyen, T.L., Castrop, E., Phung, N.A., Kieu-Le, T.C., Strady, E., Biermann, L., van der Ploeg, M., 2021. Plastic plants: the role of water hyacinths in plastic transport in tropical rivers. Frontiers in Environmental Science 9. https://doi.org/10.3389/fenvs.2021.686334.

Schreyers, L.D.M., van Emmerik, T.H.M., Bui, K., Thi, K.V.L., Vermeulen, B., Nguyen, H. Q., van der Ploeg, M., 2023. Tidal Dynamics Limit River Plastic Transport. https://doi.org/10.5194/egusphere-2022-1495.

Schwarz, A.E., Ligthart, T.N., Boukris, E., Harmelen, T.v., 2019. Sources, transport, and accumulation of different types of plastic litter in aquatic environments: a review study. Marine Pollution Bulletin 143, 92–100. https://doi.org/10.1016/j.marpolbul.2019.04.029 (publisher: Elsevier BV).

Tramoy, R., Gasperi, J., Colasse, L., Silvestre, M., Dubois, P., Noûs, C., Tassin, B., 2020a. Transfer dynamics of macroplastics in estuaries – new insights from the Seine estuary: Part 2. Short-term dynamics based on GPS-trackers. Marine Pollution Bulletin 160, 111566. https://doi.org/10.1016/j.marpolbul.2020.111566 (publisher: Elsevier BV).

Tramoy, R., Gasperi, J., Colasse, L., Tassin, B., 2020b. Transfer dynamic of macroplastics in estuaries — new insights from the Seine estuary: Part 1. Long term dynamic based on date-prints on stranded debris. Marine Pollution Bulletin 152, 110894. https://doi.org/10.1016/j.marpolbul.2020.110894 (publisher: Elsevier BV).

Valero, D., Belay, B.S., Moreno-Rodenas, A., Kramer, M., Franca, M.J., 2022. The key role of surface tension in the transport and quantification of plastic pollution in rivers. Water Research 226, 119078. https://doi.org/10.1016/j.watres.2022.119078.